Observation of wedge waves and their mode transformation by laser ultrasonic technique

Jing Jia (贾 静)*, Zhonghua Shen (沈中华), Lijuan Wang (王丽娟), and Ling Yuan (袁 玲)**

Faculty of Science, Nanjing University of Science and Technology, Nanjing 210094, China

**Corresponding author: jiasujing2@126.com; **corresponding author: shenzh@mail.njust.edu.cn*

Received July 26, 2010; accepted September 28, 2010; posted online January 28, 2011

Wedge waves (WWs) in wedges, including their dispersion characteristics and mode transformation, are investigated using the laser ultrasound technique. Pulsed laser excitation and optical deflection beam method for detection are used to record WWs. Numerous WWs are detected by scanning the excitation laser along the wedge tip. Dispersions of WWs are obtained by using the two-dimensional (2D) Fourier transformation method, and different WW orders are revealed on the wedges. Mode transformation is determined by fixing the distance between the excitation and detection position, as well as by scanning the samples along the normal direction of the wedge tip.

OCIS codes: 250.5530, 350.0350, 350.7420.

doi: 10.3788/COL201109.022501.

Wedge waves (WWs) are guided waves propagating along the tip of wedge-shaped waveguides. Lagasse *et al.* have been the first to discover this phenomenon through a numerical study in the early 1970s[1,2]. WWs have much lower velocity than Rayleigh waves, and their energy is tightly confined near the apex about of one or two wavelengths. These special characteristics enable the application of WWs in signal processing, information storage, under-water acoustics, sensors, and nondestructive detection of wedge-shaped engineering devices.

To date, there has been no elasticity-based solution capable of overcoming problems dealing with WWs. Both McKenna's thin plate theory[3] and Krylov's geometric acoustic approximation theory[4,5] have been proven valid only for small-angled wedges. Experimental work has been done to investigate the different aspects of WWs, including the influence of apex angle, apex truncation, water loading effects[6], and curvature effects of wedge apex. Jia *et al.* have been the first to use laser ultrasonic technique in studying the propagation characteristic of WWs[7,8]. Tang *et al.* have investigated the influence of wedge shape and coating on WW dispersion[9,10].

In this letter, WWs with 20° wedge, including their dispersion characteristics and modes transformation, were investigated using the laser ultrasound technique. Pulsed laser excitation and optical deflection beam method[11] for detection were employed for WW recording. Dispersions of WWs were obtained using the two-dimensional (2D) Fourier transformation method. We focused on not only the acoustic waves propagating along the tip of the wedge, but also the transformation process of wave modes along the normal direction of the wedge tip. Modes transformation by sample scanning revealed that acoustic wave energy decreases exponentially to a steady energy of Rayleigh wave within the main wavelength range.

The experimental setup is shown in Fig. 1. We excited WWs using a Q-switched Nd:YAG laser with wavelength of 1.06 μm and pulse width of 10 ns. Laser energy was maintained below the damage threshold of the specimen to ensure thermoelastic generation. A small part of the laser energy was scattered by a beam splitter and received by a photodiode as a trigger signal of the oscilloscope. In launching the acoustic waves, by using a cylinder convex lens, most of the laser energy was focused as a short line source with width of 0.5 mm on the wedge tip. This part was mounted on a translation stage to facilitate the recording of several acoustic waves at different locations. The laser source was scanned and 2D Fourier transformation method was used to analyze the modes.

A single mode He-Ne laser with 17-mW output power and 632.8-nm wavelength was employed as the source of the optical deflection beam method. This continuous laser was focused as a point source with a definite incident angle; its radius was 0.2 mm on the wedge surface. The reflected beam illuminated the center of the reflector comprising two semicircle reflectors that were tilted to a very small angle. Consequently, the detection beam was split into two beams and then focused into two photodiodes of the balanced photoreceiver (home rebuilt of New Focus model 1607-AC-FS, USA). The differential output from the balanced photoreceiver encoded the surface tilt associated with ultrasonic motion. To investigate the modes transformation of the acoustic waves, we also mounted the sample on a translation stage to allow scanning along the direction perpendicular to the propagation direction of the acoustic waves.

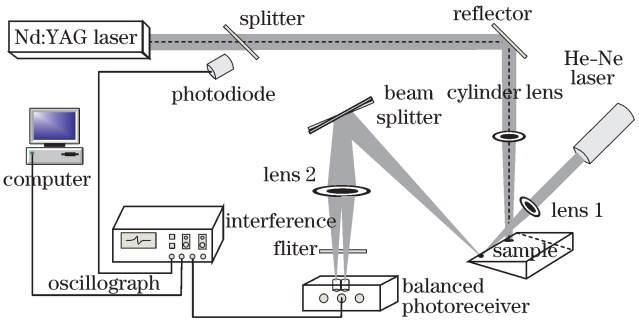

Fig. 1. Experimental setup.

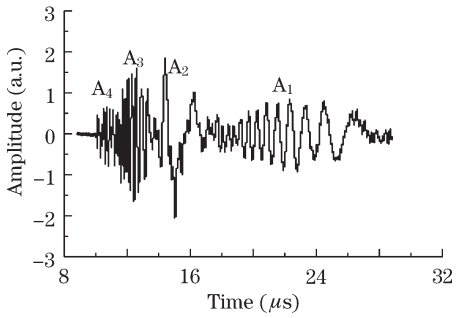

Fig. 2. WWs along the tip of the wedge with apex angle of 20°.

The WWs propagating along the tip of the wedge with an apex angle of 20° is shown in Fig. 2. Clearly, the WW is a multi-mode wave and four modes A_1, A_2, A_3, and A_4 are measured experimentally, which are nearly separated from each other in the time regime. Along the wedge tip, the WWs with a displacement field are shown as almost antisymmetric to the mid-apex plane, which are referred to as antisymmetric flexural (ASF) modes[1,7,12].

To analyze multi-modes signal in detail, we recorded the multiplied WWs by scanning the generation laser source along the wedge tip using a spatial step of 0.1 mm (Fig. 3(a)). The vertical axis denotes the propagation distance from the source; the abscissa represents time; the grayscale displays the measured slope of the surface perturbation on the wedge tip. The 2D Fourier transformation method[13,14] was employed to determine the phase velocities of WWs.

Four modes are obtained, as shown in Fig. 3(b). Lagasse's empirical formula shows that

$$v = v_{\mathrm{R}} \sin(n\theta),$$
$$n\theta < \frac{\pi}{2}, \tag{1}$$

where n is the order of ASF modes, θ is the wedge apex angle, and v_{R} is the Rayleigh wave velocity.

The expected mode numbers in this wedge with apex angle θ of 20° is exactly four. In an ideal wedge, namely, in an infinite sharp wedge, WWs are expected to be non-dispersed. The calculated phase velocities of the four modes were 1.000, 1.880, 2.533, and 2.881 km/s, respectively, with measured Rayleigh velocity of 2.925 km/s on this specimen. However, all measured velocities showed normal dispersion starting from the estimated values of Lagasse's empirical formula. Dispersion was caused by the imperfection of the wedge tip, which usually could be considered as truncated tip. We measured the truncation of the wedge by an optical microscopy. Truncation width h_0 is about 47 μm and the truncation depth of the wedge is $x_0 = \frac{h_0}{\tan\theta} \approx 0.13$ mm, as shown in Fig. 4. This apex truncation brings normal dispersion to modes A_1, A_2, and part of A_3,, all of which were within the relatively small frequency regime of approximately 0–10 MHz. The A_4 mode and high frequency range of A3 mode with wavelength range of approximately 0.2–0.3 mm propagated along the thin plate, showing similar behaviors as antisymmetric modes of Lamb waves approaching the phase velocity of a Rayleigh wave in increasing frequency.

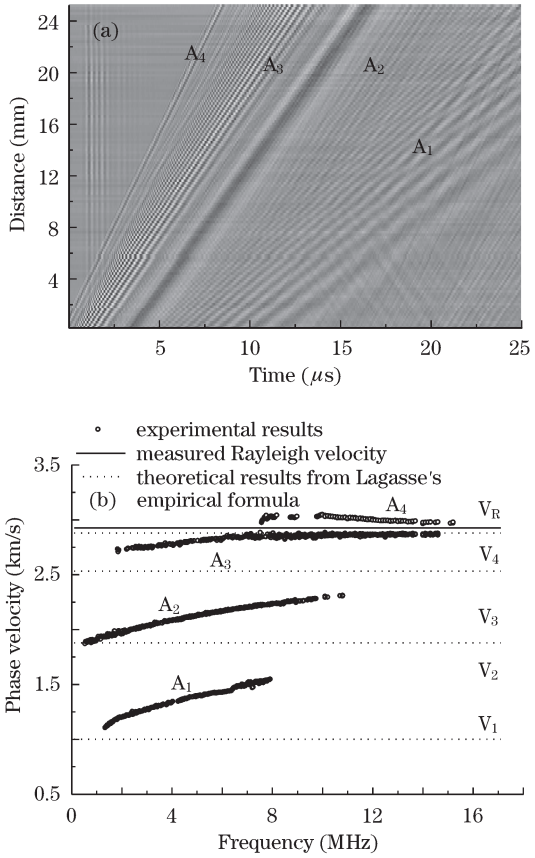

Fig. 3. (a) Space-time domain image of the multimode wedge waves and (b) their dispersion curves.

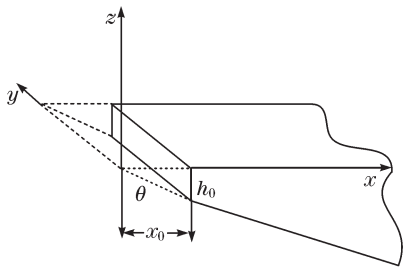

Fig. 4. Truncated wedge showing the coordinate system used. Dashed lines indicate the full wedge.

Samples were scanned with a step size of 0.05 mm along the normal direction up to the wedge tip while the position of the laser source and the detection scope were fixed. The process was conducted to determine how these modes would change when there are not confined to propagate along the wedge tip. The B-scan figure of acoustic waves on the wedge is shown in Fig. 5(a), where the vertical axis denotes the distance from the wedge tip.

WWs exhibited the strongest amplitudes near the tip. This indicates that acoustic energy is confined near the tip, and that energy is lost quickly as the propagating line is scanned away from the tip. Considering the phase velocities and frequency range of different modes, the wavelength ranges of A_2 and A_3 modes were approximately 0.2−2.5 and 0.2−1.5 mm, respectively, while those of A_1 and A_4 were about 0.2−0.6 and 0.2−0.4 mm,

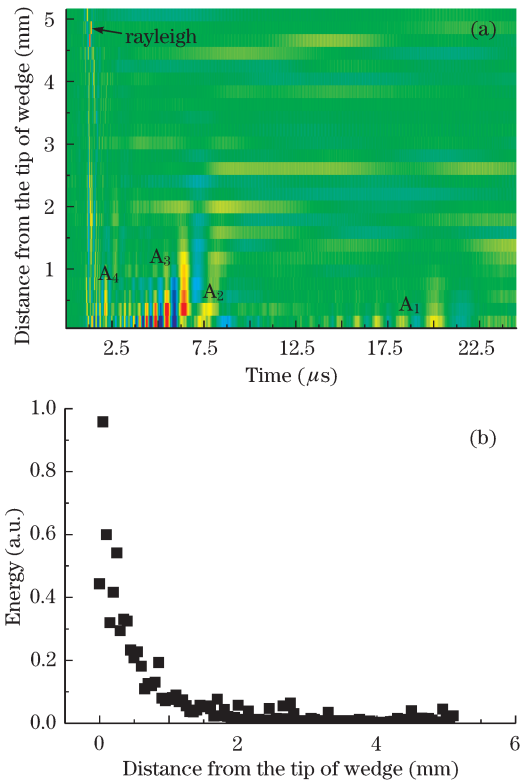

Fig. 5. (a) B-scan data in color scale of acoustic waves on the wedge surface and (b) their energy distribution.

respectively. Modes A_2 and A_3 have much relatively longer wavelengths components compared with modes A_1 and A_4. Therefore, the amplitudes of modes A_1 and A_4 decreased much faster compared with modes A_2 and A_3. Both propagating line at about 5 mm away from the tip and wedge thickness at $h = x \tan\theta \approx 2$ mm were much longer than those for the wavelength of acoustic waves. This observation demonstrates the detection of Rayleigh wave corresponding to the acoustic mode propagating along the free surface of a half space.

The energy distribution of these acoustic waves was calculated by integrating the power spectra of the acoustic waves. These values are plotted in Fig. 5(b). The wave energy decreased exponentially to a steady energy of Rayleigh wave within a distance of about 2 mm. This implies that WW energy evanesces within the wavelength range, as the main wavelength range of these modes with high signal to noise ratio is about approximately 0.2−2 mm.

In conclusion, laser excitation and optical deflection beam method for detection have been used to record WWs. The phase velocities of WWs are obtained by using the 2D Fourier transformation method. The numbers of WW modes agree with the expected values obtained from Lagasse's empirical formula; phase velocities have shown normal dispersion starting from the estimated values of the said formula. Dispersion might have been caused by the imperfection of the wedge tip. We have focused on not only acoustic waves propagating along the tip of the wedge, but also the transformation process of wave modes along the normal direction up to the wedge tip. Results have shown that the energy of acoustic waves decrease exponentially to a steady energy of Rayleigh wave within the main wavelength range of acoustic modes.

This work was supported by the National Natural Science Foundation of China (Nos. 60778006 and 60878023) and the Teaching and Research Award Program for Outstanding Young Professor in Higher Education Institute, Ministry of Education, China.

References

1. P. E. Lagasse, Electron. Lett. **8,** 372 (1972).
2. P. E. Lagasse, I. M. Mason, and E. A. Ash, IEEE Trans. Microw. Theory **Mt21,** 225 (1973).
3. J. Mckenna, G. D. Boyd, and R. N. Thurston, IEEE Trans. Sonics Ultr. **Su21,** 178 (1974).
4. V. V. Krylov, in *Proceedings of 1994 IEEE Ultrasonics Symposium* **1-3,** 793 (1994).
5. V. V. Krylov, J. Acoust. Soc. Am. **103,** 767 (1998).
6. V. V. Krylov and G. V. Pritchard, Applied Acoustics **68,** 97 (2007).
7. X. Jia and M. de Billy, Appl. Phys. Lett. **61,** 2970 (1992).
8. D. Auribault, X. Jia, M. Debilly, and G. Quentin, J. Phys. Iv **4,** 737 (1994).
9. S.-W. Tang and C.-H. Yang, IEEE Trans. Ultrason. Ferroelectr. Freq. Control **55,** 2674 (2008).
10. C.-H. Yang and C.-Z. Tsen, IEEE Trans. Ultrason. Ferroelectr. Freq. Control **53,** 754 (2006).
11. Y. Shi, Z. Shen, X. Ni, and J. Lu, Proc. SPIE **6825,** 682511 (2007).
12. I. M. Mason, R. M. Delarue, R. V. Schmidt, E. A. Ash, and P. E. Lagasse, Electron. Lett. **7,** 395 (1971).
13. X. Zhou and H. Zhao, Acta Opt. Sin. (in Chinese) **29,** 1563 (2009).
14. L. Yuan, X. Ren, G. Yan, Z. Shen, X. Ni, J. Lu, and Y. Zhang, Chinese J. Lasers (in Chinese) **35,** 120 (2008).